

Optimal Choice for Number of Strands in a Litz-Wire Transformer Winding

Charles R. Sullivan, *Member, IEEE*

Abstract—The number and diameter of strands to minimize loss in a litz-wire transformer winding is determined. With fine stranding, the ac resistance factor can be decreased, but dc resistance increases as a result of the space occupied by insulation. A power law to model insulation thickness is combined with standard analysis of proximity-effect losses to find the optimal stranding. Suboptimal choices under other constraints are also determined.

Index Terms—Eddy currents, litz wire, magnet wire, power electronics, power transformers, proximity-effect losses, skin effect, transformer windings.

I. INTRODUCTION

A SALIENT difficulty in the design of high-frequency inductors and transformers is eddy-current effects in windings. These effects include skin-effect losses and proximity-effect losses. Both effects can be controlled by the use of litz wire—conductors made up of multiple individually insulated strands twisted or woven together. (Sometimes the term *litz wire* is reserved for conductors constructed according to a carefully prescribed pattern, and strands simply twisted together are called bunched wire. We will use the term *litz wire* for any insulated grouped strands.)

This paper addresses the choice of the degree of stranding in litz wire for a transformer winding. The number of turns and the maximum winding cross-sectional area are assumed to be fixed. Under constraints on maximum number of strands or minimum wire diameter, the best solution may not fill the allocated window space fully. However, as will be shown in Section IV, with those constraints removed, the optimum solution does fill the allocated space. In this case, the cross-sectional area of each turn is fixed, and as the number of strands is increased, the cross-sectional area of each strand must be decreased. This typically leads to a reduction in eddy-current losses. However, as the number of strands increases, the fraction of the window area that is filled with copper decreases and the fraction filled with insulation increases. This results in an increase in dc resistance. Eventually, the eddy-current losses are made small enough that the increasing dc resistance offsets any further improvements in eddy-current loss, and the total losses start to increase. Thus, there is an optimal number of strands that results in minimum loss.

This paper presents a method of finding that optimum, using standard methods of estimating the eddy-current losses.

Optimizations on magnetics design may be done to minimize volume, loss, cost, weight, temperature rise, or some combination of these factors. For example, in the design of magnetic components for a solar-powered race vehicle [1] (the original impetus for this work) an optimal compromise between loss and weight is important. Although we will explicitly minimize only winding loss, the results are compatible with and useful for any minimization of total loss (including core loss), temperature rise, volume, or weight. This is because the only design change considered is a change in the degree of stranding, preserving the overall diameter per turn and overall window area usage. This does not affect core loss or volume and has only a negligible effect on weight. However, the degree of stranding does significantly affect cost. Although we have not attempted to quantify or optimize this, additional results presented in Section V are useful for cost-constrained designs.

The analysis of eddy-current losses used here does not differ substantially from previous work [2]–[18] ([15] gives a useful review). Although different descriptions can be used, most calculations are fundamentally equivalent to one of three analyzes. The most rigorous approach uses an exact calculation of losses in a cylindrical conductor with a known current, subjected to a uniform external field, combined with an expression for the field as a function of one-dimensional (1-D) position in the winding area [17]. Perhaps the most commonly cited analysis [16] uses “equivalent” rectangular conductors to approximate round wires and then proceeds with an exact 1-D solution. Finally, one may use only the first terms of a series expansion of these solutions, e.g., [14].

All of these methods give similar results for strands that are small compared to the skin depth [17]. (See Appendix B for a discussion of one minor discrepancy.) The solutions for optimal stranding result in strand diameters much smaller than a skin depth. In this region, the distinctions between the various methods evaporate, and the simplest analysis is adequate. More rigorous analysis (e.g., [17]) is important when strands are not small compared to a skin depth. In this case, losses are reduced relative to what is predicted by the analysis used here, due to the self-shielding effect of the conductor.

Previous work, such as [2]–[9] has addressed optimal wire diameter for single-strand windings. The approach in [2]–[9] is also applicable for litz-wire windings in the case that the number of strands is fixed, and the strand diameter for lowest loss is desired [5], [9]. As discussed in Section V, this can be

Manuscript received August 28, 1997; revised July 6, 1998. Recommended by Associate Editor, J. Sarjeant.

The author is with the Thayer School of Engineering, Dartmouth College, Hanover, NH 03755-8000 USA.

Publisher Item Identifier S 0885-8993(99)01828-1.

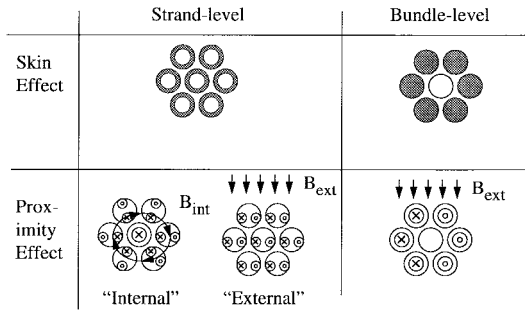


Fig. 1. Types of eddy-current effects in litz wire.

useful for cost-sensitive applications if the number of strands is the determining factor in cost and the maximum cost is constrained. However, this will, in general, lead to higher loss designs than are possible using the optimal number of strands.

II. SKIN EFFECT AND PROXIMITY EFFECT IN LITZ WIRE

Skin effect is the tendency for high-frequency currents to flow on the surface of a conductor. Proximity effect is the tendency for current to flow in other undesirable patterns—loops or concentrated distributions—due to the presence of magnetic fields generated by nearby conductors. In litz-wire windings, skin and proximity effects may be further divided into strand-level and bundle-level effects, as illustrated in Fig. 1. Bundle-level effects relate to current circulating in paths involving multiple strands, whereas strand-level effects take place within individual strands. Bundle-level effects are controlled by the pattern of twisting or weaving—the construction of the litz wire. Simple twisting is adequate to control bundle-level proximity effect loss, whereas more complex constructions are needed to control bundle-level skin effect. Bundle-level effects are not directly affected by the number or diameter of strands; they are determined by the overall diameter and the choice of twisting pattern. Thus, they need not be considered further for the analysis in this paper. At the strand level, proximity effect dominates skin effect in a winding that has many layers. Since a litz winding has a large effective number of layers as a result of the many strands, strand-level skin effects are negligible.

Thus, we need only consider strand-level proximity effect losses for the choice of number of strands. Strand-level proximity effect may be still further divided into internal proximity effect (the effect of other currents within the bundle) and external proximity effect (the effect of current in other bundles) [19], [20]. However, this distinction is useful only as a form of bookkeeping. The actual losses in one strand of a litz bundle are simply a result of the total external field, due to the currents in all the other strands present.

To calculate the total strand-level proximity-effect loss in a litz winding, one can view it as a single winding, made up of nN turns of the strand wire, each with current i/n flowing in it, where n is the number of strands, N is the number of turns of litz wire, and i is current flowing in the overall litz bundle. The loss in the litz winding will be the same as in the equivalent single-strand winding as long as the currents flowing in all the strands are equal [6], [21]. Other methods of calculating loss in litz wire also assume

equal current in all strands [17], [19], [22]. This assumption is equivalent to assuming that the bundle-level construction has been chosen properly to control bundle-level proximity and skin effects. Note, however, that most of our results remain valid even when there is significant skin-effect loss at the litz-bundle level, for example in a simply twisted bundle. This is because the bundle-level skin-effect loss is independent of the number of strands, and is orthogonal [20] to the strand-level eddy-current losses.

We represent winding losses by

$$P_{\text{loss}} = F_r I_{\text{ac}}^2 R_{\text{dc}} \quad (1)$$

where F_r is a factor relating dc resistance to an ac resistance which accounts for all winding losses, given a sinusoidal current with rms amplitude I_{ac} . As shown in Appendix A, we can approximate F_r by

$$F_r = 1 + \frac{\pi^2 \omega^2 \mu_0^2 N^2 n^2 d_c^6 k}{768 \rho_c^2 b_c^2} \quad (2)$$

where ω is the radian frequency of a sinusoidal current, n is the number of strands, N is the number of turns, d_c is the diameter of the copper in each strand, ρ_c is the resistivity of the copper conductor, b_c is the breadth of the window area of the core, and k is a factor accounting for field distribution in multiwinding transformers, normally equal to one (see Appendix A). For waveforms with a dc component, and for some nonsinusoidal waveforms, it is possible to derive a single equivalent frequency that may be used in this analysis (Appendix C). In an inductor, the field in the winding area depends on the gapping configuration, and this analysis is not directly applicable [23].

The analysis described here considers the strands of all litz bundles to be uniformly distributed in the window, as they would be in a single winding using Nn turns of wire the diameter of the litz strands. In fact, the strands are arranged in more or less circular bundles. In this sense, the analysis of [20] may be more accurate, but this difference has very little effect on the results. The most important difference between the model used here and the model in [20] is the greater accuracy of [20] for strands that are large compared to a skin depth. The simpler model is used because it is accurate for the small strand diameters that are found to be optimal, and because its simplicity facilitates finding those optimal diameters. Other models (such as [19] and the similar analysis in [22]) also model large strand diameters and circular bundle configurations accurately, but they fully calculate only internal (not external) proximity effect, and so are not useful for the present purposes.

III. DC RESISTANCE FACTORS

The fraction of the window area occupied by copper in a litz-wire winding will be less than it could be with a solid-wire winding. This leads to higher dc resistance than that of a solid wire of the same outside diameter. A cross section of litz wire is shown in Fig. 2, with the various contributions to cross-sectional area marked. In addition to the factors shown in this diagram, the twist of the litz wire also increases the

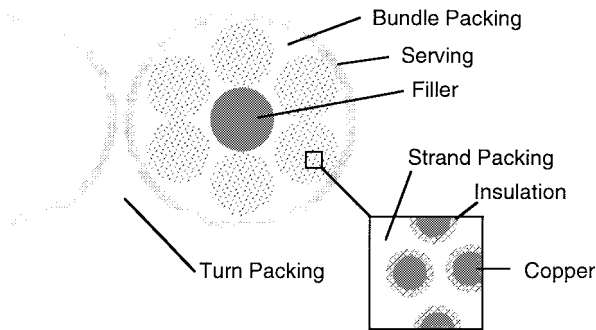


Fig. 2. Cross-sectional area of a litz-wire winding showing how area is allocated. Area allocated to anything other than copper increases the resistance in a space-limited winding.

dc resistance. In order to find the optimal number of strands for a litz winding, it is necessary to quantify how the factors affecting dc resistance vary as a function of the number of strands.

A. Serving

Typically, litz bundles are wrapped with textile to protect the thin insulation of the individual strands. This serving adds about 0.06 mm (2.5 mil) to the diameter of the bundle. For a given number of turns filling a bobbin, or a section of a bobbin, the outside diameter of the litz wire must be fixed. The area devoted to serving will then also be fixed, independent of the number of strands.

B. Strand Packing

Simply twisted litz wire comprises a group of strands bunched and twisted into a bundle. More complex constructions begin with this step, and then proceed with grouping and twisting the subbundles into higher level bundles. Particular numbers of strands (1, 7, 19, 37, etc.) pack neatly into concentric circular arrangements. However, with large numbers of strands (e.g., >19), and/or very fine strands [e.g., 44–50 American Wire Gauge (AWG)], it is difficult to precisely control the configuration, and the practical packing factor becomes an average number approximately independent of the number of strands. Since the optimal strand diameter is typically much smaller than a skin depth, but the lowest level bundle can be near a skin depth in diameter, in most cases we can assume that there is a large number of strands in the innermost bundle. Thus, this packing factor is independent of the number of strands.

C. Bundle Packing and Filler

The way the strands are divided into bundles and subbundles is chosen based on considerations including bundle-level skin-effect losses, flexibility of the overall bundle, resistance to unraveling, and packing density. In some cases, a nonconducting filler material may be used in the center of a bundle in place of a wire or wire bundle that would, in that position, carry no current because of skin effect.

A typical configuration chosen to avoid significant bundle-level skin-effect losses should have a carefully designed and

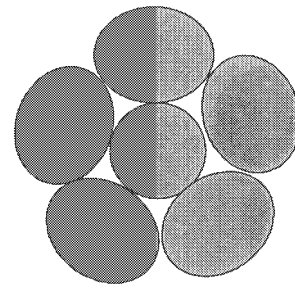


Fig. 3. The cross section of strands becomes elliptical when the bundle is twisted. In this extreme case of lay (length per twist) equal to 4.7 times the bundle diameter, a total of six strands fit where seven would have fit untwisted.

potentially complex construction at the large-scale level where bundle diameters are large compared to a skin depth. However, because the optimal strand diameter will be small compared to a skin depth, a simple many-strand twisted bundle may be used at the lowest level. If the overall number of strands is increased, the number of strands in each of these low-level bundles should be increased, but the diameter of each low-level bundle should not be changed, nor should the way they are combined into the higher level construction be affected. Thus, for our purposes, the bundle packing factor is independent of the number of strands.

D. Turn Packing

The way turns are packed into the overall winding is primarily a function of winding technique, and it is assumed not to vary as a function of the stranding. However, note that loosely twisted litz wires can deform as the winding is constructed, allowing tighter packing. Another option providing tight turn packing is rectangular-cross-section litz wire. In addition to its turn-packing advantage, it has tighter strand and bundle packing, as a result of the mechanical compacting process that forms it into a rectangular cross section.

E. Twist

The distance traveled by a strand is greater in a twisted bundle than it would be if the strands simply went straight, and so the resistance is greater. An additional effect arises from the fact that a cross section perpendicular to the bundle cuts slightly obliquely across each strand. Thus, the cross section of each strand is slightly elliptical. This reduces the number of strands that fit in a given area, and so effectively increases the resistance. An extreme case of this is illustrated in Fig. 3. The choice of the pitch of the twist (“lay” or length per twist) is not ordinarily affected by the number of strands in the lowest level bundle, and so for the purpose of finding the optimal number of strands, we can again assume it is constant.

F. Strand Insulation Area

Thinner magnet wire has thinner insulation. However, the thickness of the insulation is not in direct proportion to the wire diameter. Thinner wire has copper in a smaller fraction of the overall cross-sectional area and insulation in a larger fraction.

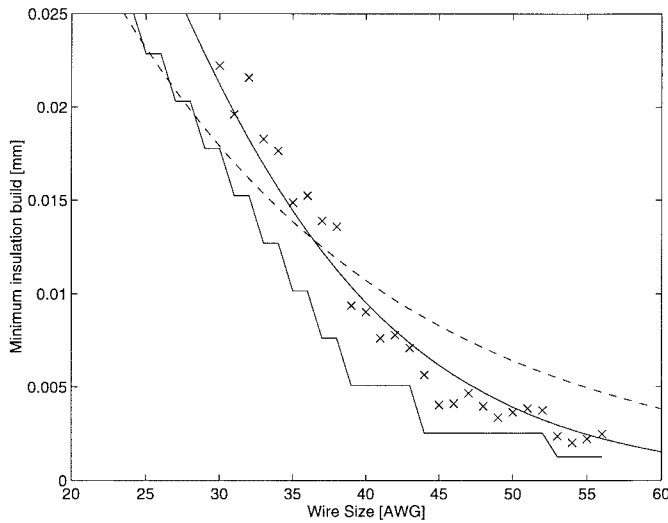


Fig. 4. Insulation build (twice the insulation thickness) for AWG single-build magnet wire. The dashed curve is the minimum build according to the equation provided by [24]. The lower “staircase” curve is the tabulated data provided by [24] for minimum build. The points marked by “x” are nominal build from a wire manufacturer’s catalog obtained by subtracting an exact theoretical nominal wire diameter from the tabulated nominal overall diameter. The approximation described by (4) comes closest to these points.

Of all of the dc-resistance factors considered, this is the only one that varies with the size or number of strands used at the lowest level of the construction. Thus, quantifying this effect on dc resistance gives a good approximation of the total variation in dc resistance as a function of the size or number of strands. The other factors can be lumped into an overall dc resistance multiplying factor which is a constant for the present purposes.

One approach to quantifying the relationship between the insulation area and strand diameter would be to store tables in computers, and use them to find the optimal strand diameter by calculating the losses for different strand diameters until the optimum was found, similar to [11]. However, an analytical description of the variation of insulation thickness with wire size can facilitate an analytical solution for the optimal number of strands.

An equation describing magnet wire insulation thickness is provided by [24]

$$\log_{10} B = X - \frac{\text{AWG}}{44.8} \quad (3)$$

where B is the minimum insulation build in mils (10^{-3} in, 1 mil = $25.4 \mu\text{m}$), $X = 0.518$ for single-build insulation and $X = 0.818$ for heavy (double) build, and AWG is the American Wire Gauge number.¹ However, this only applies to wire sizes between 14 and about 30 AWG. For smaller wire sizes, it does not correlate with the tabulated data in [24] (Fig. 4). For wire in the range of 30–60 AWG, we find a better fit to manufacturers’ tabulated nominal insulation build by using

$$d_t = d_r \alpha \left(\frac{d_c}{d_r} \right)^\beta \quad (4)$$

¹The American wire gauge defines nominal wire diameter in inches as $d = 0.0050(92)^{(36-\text{AWG})/39}$.

where d_t is the overall diameter, including the insulation thickness, d_c is the diameter of the copper only, and d_r is an arbitrarily defined reference diameter used to make the constants α and β unitless. The parameters found for single-build insulation wire are $\beta = 0.97$ and $\alpha = 1.12$ for d_r chosen to be the diameter of AWG 40 wire (0.079 mm). For heavy-build insulation, $\beta = 0.94$ and $\alpha = 1.24$. Note that although (4) provides an accurate approximation for wire in the range of 30–60 AWG, its asymptotic behavior for large-strand diameters is pathological. Insulation thickness goes to zero around 6 AWG and is negative for larger strands.

IV. NUMBER OF STRANDS FOR MINIMUM LOSS

With no constraints on number of strands or strand diameter, the minimum-loss design will be with a full bobbin. Any design that does not fill the bobbin can be improved by increasing the number of strands by a factor s , and decreasing the strand diameter d_c by $1/\sqrt{s}$. This keeps the dc resistance constant and decreases ac resistance, as shown by (2). This improvement can be continued until insulation area increases result in a full bobbin. Thus, the minimum-resistance solution fills the bobbin, and we can find this solution by analyzing a full bobbin.

For a full bobbin, the outside diameter of the complete litz bundle is

$$d_{tl} = \sqrt{\frac{F_p b_b h}{N}} \quad (5)$$

where b_b is the breadth of the bobbin, h is the height allocated for the particular winding under consideration, N is the number of turns in that winding, and F_p is a turn-packing factor for turns in the winding, expressed relative to perfect square packing (for $F_p = 1$, the litz bundle would occupy $\pi/4$ of the window area).

Assuming a factor F_{lp} accounting for serving area, bundle packing, any filler area, strand packing, and the effect of twist on diameter, we can find the outside diameter of a single strand

$$d_t = \sqrt{\frac{F_p F_{lp} b_b h}{nN}} \quad (6)$$

where n is the number of strands in the overall litz bundle.

The diameter of the copper in a single strand can then be written using (4)

$$d_c = d_r^{1-1/\beta} \alpha^{-1/\beta} \left(\frac{F_p F_{lp} b_b h}{nN} \right)^{1/(2\beta)} \quad (7)$$

We now define a total resistance factor F_r'

$$F_r' = F_{dc} F_r = \frac{\text{ac resistance of litz-wire winding}}{\text{dc resistance of single-strand winding}} \quad (8)$$

where F_{dc} is the ratio of dc resistance of the litz wire to the dc resistance of a single strand winding, using wire with the same diameter as the litz-wire bundle. Using (6) and (7), we can show

$$F_{dc} = n^{1/\beta-1} F_{lp}^{-1/\beta} \quad (9)$$

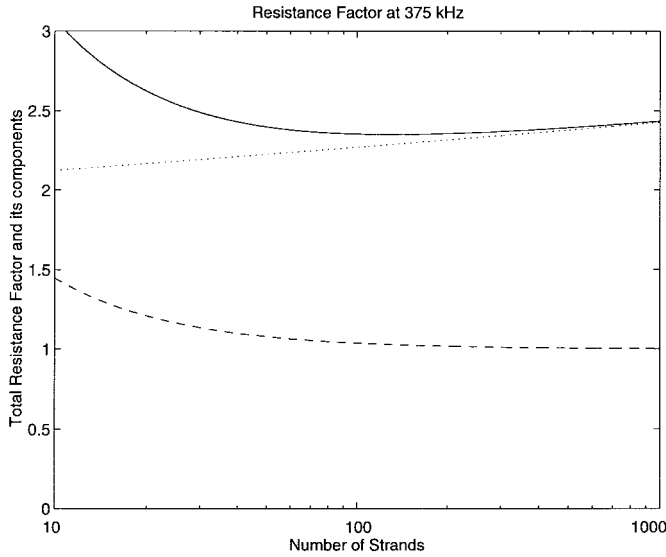


Fig. 5. Total resistance factor F_r' as a function of number of strands (solid line) for the example discussed in the text at 375 kHz. Also shown are the ac resistance factor F_r (dashed) and the dc resistance factor F_{dc} (dotted). The minimum total resistance factor is at the point where increases in F_{dc} balance decreases in F_r with an increasing number of strands.

Combining (2), (8), and (9) results in

$$F_r' = F_{lp}^{-1/\beta} [n^{1/\beta-1} + \gamma n^{(1-2/\beta)}] \quad (10)$$

where

$$\gamma = \frac{\pi^2 N^2 \omega^2 \mu_0^2 d_r^{6-6/\beta} \alpha^{-6/\beta} (F_p F_{lp} b_b h / N)^{3/\beta} k}{768 \rho_c^2 b_c^2}. \quad (11)$$

Equation (10) can now be minimized with respect to n to find the optimal number of strands

$$n_{opt} = \left(\frac{(2/\beta - 1)\gamma}{1/\beta - 1} \right)^{1/(3/\beta - 2)}. \quad (12)$$

This will give nonintegral numbers of strands; the nearest integral number of strands can be chosen to minimize ac resistance.

V. DESIGN EXAMPLES AND SUBOPTIMAL STRANDING

For a design example, we used a 14-turn winding on an RM5-size ferrite core. The breadth of the bobbin is 4.93 mm, and the breadth of the core window 6.3 mm. A height of 1.09 mm is allocated to this winding. Based on an experimental hand-wound packing factor $F_p = 0.85$ and litz packing factor $F_{lp} = 0.66$, unserved, plus a 32- μm (1.25 mil) layer of serving, the above calculation indicates that, for a frequency of 375 kHz, 130 strands of number 48 wire gives minimum ac resistance, with a total resistance factor of $F_r' = 2.35$, ac resistance factor $F_r = 1.03$, and a dc resistance factor $F_{dc} = 2.29$.

Fig. 5 shows the total calculated resistance factor and its components as a function of number of strands. The figure and the numbers confirm the intuition that because β is close to one and the dc resistance increases only very slowly, the decrease in resistance using finer strands outweighs the decreased cross-sectional area until the ac resistance factor is brought very

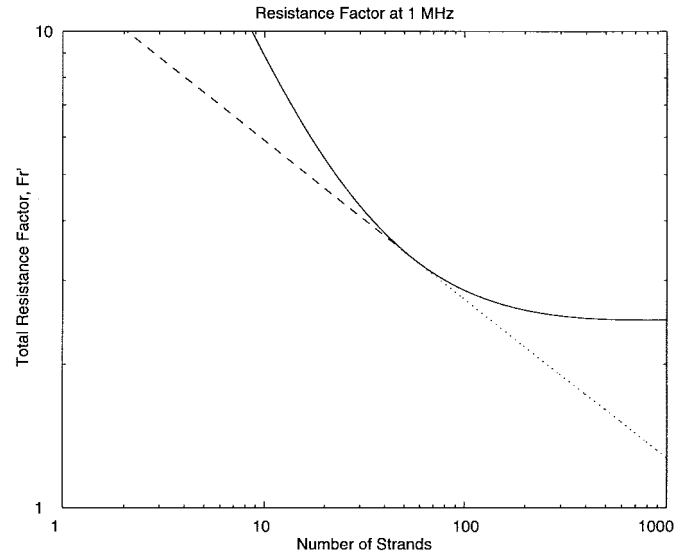


Fig. 6. Total resistance factor F_r' as a function of number of strands for the example discussed in the text at 1 MHz. The solid line indicates resistance factor for a full bobbin. The dashed line shows the lower resistance that is possible by choosing the strand diameter for minimum loss, with the number of strands fixed. Where this optimal diameter results in a full bobbin, the two curves are tangent. For larger numbers of strands, the optimal strand diameter, shown as a dotted line, would overfill the bobbin and so is not possible.

close to one. Note that although the factor F_{dc} is large, only a factor of 1.18 is due to the change in wire insulation thickness. The remaining factor of 1.95 is due to the dc resistance factors that do not vary with number of strands, such as serving area and strand packing.

The optimization leads to choosing a large number of fine strands, which will often mean a high cost, and will sometimes require finer strands than are commercially available. From Fig. 5, one can see that a decrease from the optimum of 130 to about 50 strands entails only a small increase in ac resistance. Consideration of the cost tradeoff for a particular application becomes necessary.

Given a suboptimal number of strands, chosen to reduce costs, a full bobbin may no longer be best. The problem of choosing the optimal strand diameter for a fixed number of strands has been addressed by many authors [2]–[5], [7]–[9], [14]. Although this is typically only used for single strands, the analysis also can be applied for more than one strand by simply using the product of the number of turns and the number of strands Nn in place of the number of turns N . The result [7]–[9], [14] that $F_{r_{opt}} = 1.5$ holds, and

$$d_{opt} = \left(\frac{384 \rho_c^2 b_c^2}{\pi^2 \omega^2 \mu_0^2 N^2 n^2} \right)^{1/6}. \quad (13)$$

In many practical cases, cost is a stronger function of the number of strands than of the diameter of the strands. In the range of about 42–46 AWG, the additional manufacturing cost of smaller wire approximately offsets the reduced material cost. Thus, designs using the diameter given by (13) often approximate the minimum ac resistance for a given cost.

Fig. 6 shows total resistance factor as a function of the number of strands for the same example design, but at 1 MHz, where the optimal stranding is a difficult and expensive 792

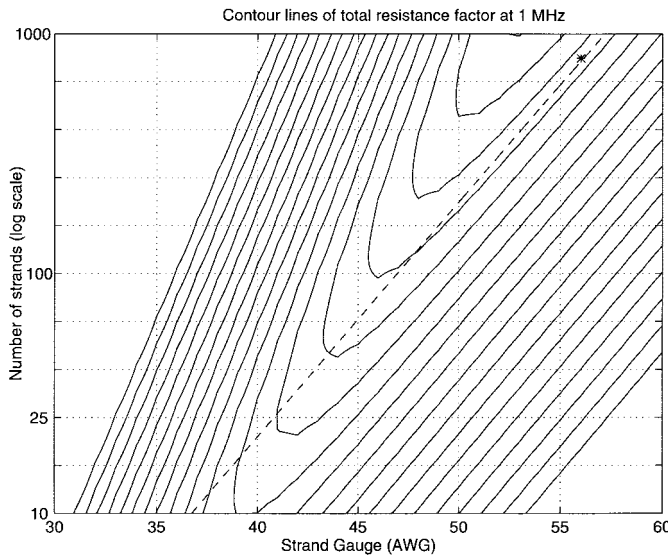


Fig. 7. Contour lines of total resistance factor F_r' as a function of number of strands and diameter of strands for the example discussed in the text at 1 MHz. The diagonal dashed line indicates a full bobbin. The valley at the upper right is the minimum loss. The minimum loss without overfilling the bobbin is marked by an "x." Contour lines are logarithmically spaced.

strands of AWG 56 wire, and so analysis of alternatives is more important. The solid line is for a full bobbin, and the dashed line is for the same number of strands, but with the diameter chosen for minimum losses rather than to fill the bobbin. Where the two lines meet, the optimal diameter just fills the bobbin. Beyond that point it would not fit, and the line is shown dotted.

The example can be understood more completely by examining contour lines of total resistance factor F_r' as a function of both strand diameter and number of strands (Fig. 7). The minimum resistance is in the valley at the upper right (a large number of fine strands). To fit on the bobbin, designs must be below the dashed diagonal line. Minimum loss designs for a fixed number of strands can be found by drawing a horizontal line for the desired number of strands, and finding the point tangent to contour lines.

One could also consider a constraint for minimum wire diameter. Many manufacturers cannot provide litz wire using strands finer than 48 or 50 AWG. In Fig. 7, the minimum resistance for 50 AWG stranding is with a full bobbin, but for 40-AWG wire, the minimum ac resistance can be seen to occur with fewer than the maximum number of strands. This situation can be analyzed by considering (2) with all parameters fixed except for the number of strands, such that

$$F_r = 1 + \zeta n^2 \quad (14)$$

where ζ is a constant obtained by equating (2) and (14). The total resistance factor is then

$$F_r' = F_{dc1} \cdot (1 + \zeta n^2)/n \quad (15)$$

where F_{dc1} is the dc resistance factor with a full bobbin, for the fixed strand diameter. The value of n that minimizes this expression is $n = \sqrt{1/\zeta}$, such that $F_r = 2$. This will be the optimal number of strands, given a fixed minimum strand

diameter, unless this is too many strands to fit in the available window area.

The above analysis shows how to find the optimal stranding, given a constraint on either strand diameter or number of strands, both of which are important in determining cost. More explicit analysis of cost is addressed in [25].

VI. EXPERIMENTAL RESULTS

The designs specified in the preceding section were constructed with two types of litz wire: 130 strands of 48 AWG and 50 strands of 44 AWG. The primary and secondary windings were made from a single length of litz wire, wound on the bobbin in opposite directions. This is magnetically equivalent to having a shorted secondary, but it reduces potential problems with interconnect resistance. In order to evaluate skin effect in the absence of external proximity effect, litz wire was also measured outside of a winding. The resistance was measured with an HP 4284A LCR meter, using a custom-built test jig for low-impedance measurements. The measurements are shown in Fig. 8.

Although the overall litz-wire diameter was small enough to limit bundle-level skin-effect losses to a few percent, the fine strands in the optimal solution also limit proximity-effect losses to similar levels, so it is necessary to separate the two effects in order to judge the accuracy of the proximity-effect calculations. Fortunately, the losses are orthogonal [20], and the skin effect losses (for a litz wire outside of the winding) can simply be subtracted from the measured losses in the transformer in order to isolate proximity-effect losses. Accurate prediction of the bundle-level skin effect was found to be difficult, in part because the details of the bundle constructions were not well known. However, if the experimentally measured bundle-level skin effect is subtracted from the total measured losses, the result matches the proximity-effect losses predicted by (2) very closely, as can be seen in Fig. 8. This confirms the validity of the model used in the optimization.

VII. CONCLUSION

The number of strands for a minimum-loss litz-wire winding may be found by evaluating the tradeoff between proximity-effect losses and dc resistance. Of the factors leading to increased dc resistance in a litz-wire winding, only the space allocated to strand insulation varies significantly with the number of strands in a well designed construction. A power law can be used to model insulation thickness in the region of interest. Combining this with standard models for eddy-current loss results in an analytic solution for the optimal number of strands. The simplest model for loss, using only the first terms of a series expansion, can be used because good designs use strands that are small compared to a skin depth. Experimental results correlate well with the simple model.

Stranding for minimum loss may lead to many strands of fine wire and thus excessive expense. Minimum loss designs constrained by minimum strand size or maximum number of strands have also been derived.

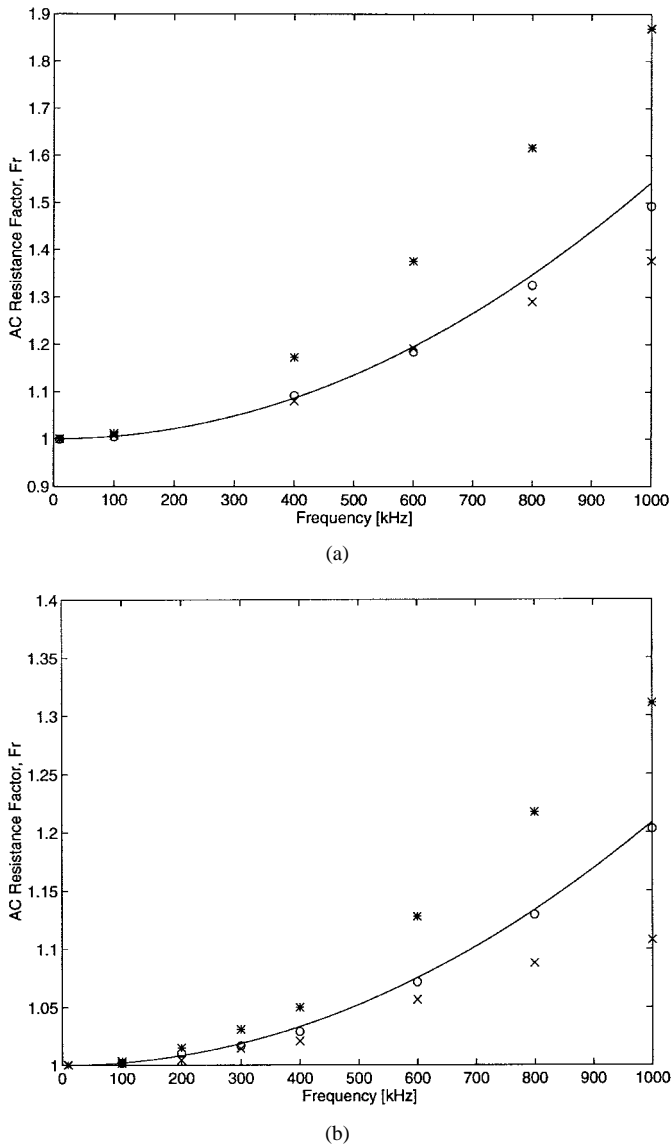


Fig. 8. Experimental ac resistance factor F_r as a function of frequency. (a) Graph is for litz wire with 50 strands of 44 AWG wire. (b) Graph is 130 strands of 48 AWG wire. Both are in the example transformer described in the text. Total measured resistance factor in the transformer is marked with stars. Measured skin effect in a straight piece of litz wire is marked with “x.” The difference, equal to proximity-effect losses, is marked with circles. These correspond closely to the predicted proximity-effect losses (solid line).

APPENDIX A LOSS CALCULATION

The expression for ac resistance factor F_r used here may be derived by first calculating loss in a conducting cylinder in a uniform field, with the assumption that the field remains constant inside the conductor, equivalent to the assumption that the diameter is small compared to a skin depth. This results in power dissipation P in a wire of length ℓ

$$P = \frac{\pi\omega^2\ell B^2 d_c^4}{128\rho_c} \quad (16)$$

where B is the peak flux density. This is equal to the first term of an expansion of the exact Bessel-function solution [26].

Combining this with the assumption of a trapezoidal field distribution results in (2). For configurations in which the

field is not zero at one edge of the winding, a factor $k = (1 - \varphi^3)/(1 - \varphi)^3$ is used to account for the resulting change in losses, where $\varphi = B_{\min}/B_{\max}$ [14].

APPENDIX B

COMPARISON WITH EXPANSION OF DOWELL SOLUTION

Equation (2) is similar to the expression for the first terms of a series expansion of the exact one-dimension solution

$$F_r = 1 + \frac{5p^2 - 1}{45} \psi^4 \quad (17)$$

where p is the number of layers and ψ is the ratio of effective conductor thickness to skin depth. For a large number of layers (equivalent to the assumption, given above, of a trapezoidal field distribution), this reduces to $F_r = 1 + (p^2/9) \psi^4$. The usual expression for ψ is

$$\psi = \sqrt{F_l} h_{\text{eq}}/\delta \quad (18)$$

where $F_l = N_l b_{\text{eq}}/b_b h_{\text{eq}}$ and b_{eq} are the height and breadth of an “equivalent” rectangular conductor and N_l is the number of turns per layer. Based on equal cross-sectional area, $b_{\text{eq}} = h_{\text{eq}} = \sqrt{\pi/4} d_c$. This results in

$$\psi^4 = \frac{(\pi/4)^3 d_c^6 N n}{\delta^4 b_b h_b} \quad (19)$$

where h_b is the height of the bobbin area allocated to this winding. The number of layers is $p = \sqrt{n N h_b / b_b}$. Substituting these expressions for p and ψ into the simplified version of (17) and using $\delta = \sqrt{2\rho_c / (\mu_0 \omega)}$, we obtain

$$F_r = 1 + \frac{\pi^3 \omega^2 \mu_0^2 N^2 n^2 d_c^6 k}{3 \cdot 768 \rho_c^2 b_b^2} \quad (20)$$

the same as (2), except for the substitution of b_b for b_c and the addition of a factor of $\pi/3$. This discrepancy, which was first noted in [6], can be explained by comparing (16) to the equivalent expression for a rectangular conductor

$$P = \frac{\omega^2 \ell B^2 s^4}{24\rho_c} \quad (21)$$

where s is the side of a square conductor. Equating these two, we obtain $s = (3\pi/16)^{1/4} d_c$. Thus, it appears that using an equivalent square conductor with sides equal to $s = (3\pi/16)^{1/4} d_c$ for proximity-effect loss calculations would be a more accurate approximation than the equal area approximation that is usually used [16].

APPENDIX C

NONSINUSOIDAL CURRENT WAVEFORMS

Nonsinusoidal current waveforms can be treated by Fourier analysis. The current waveform is decomposed into Fourier components, the loss for each component is calculated, and the loss components are summed to get the total loss

$$P = \sum_{j=0}^{\infty} I_j^2 F_r(\omega_j) R_{\text{dc}} \quad (22)$$

where I_j is the rms amplitude of the Fourier component at frequency ω_j . From (2), it can be seen that

$$F_r(\omega) = 1 + (F_R(\omega_1) - 1) \frac{\omega^2}{\omega_1^2}. \quad (23)$$

Defining $F_{r\text{-tot}}$ by $P = I_{\text{tot-rms}}^2 F_{r\text{-tot}} R_{\text{dc}}$ leads to

$$F_{r\text{-tot}} = 1 + \frac{(F_r(\omega_1) - 1) \sum_{j=0}^{\infty} I_j^2 \frac{\omega_j^2}{\omega_1^2}}{I_{\text{tot-rms}}^2}. \quad (24)$$

This can also be written as

$$F_{r\text{-rms}} = 1 + (F_R(\omega_1) - 1) \frac{\omega_{\text{eff}}^2}{\omega_1^2} \quad (25)$$

where

$$\omega_{\text{eff}} = \sqrt{\frac{\sum_{j=0}^{\infty} I_j^2 \omega_j^2}{\sum_{j=0}^{\infty} I_j^2}}. \quad (26)$$

One may calculate this effective frequency for a nonsinusoidal current waveform and use it for analysis of litz-wire losses, or for other eddy-current loss calculations. Note that this applies to waveforms with dc plus sinusoidal or nonsinusoidal ac components. The results will be accurate as long as the skin depth for the highest important frequency is not small compared to the strand diameter.

A triangular current waveform with zero dc component results in an effective frequency of $1.103\omega_1$, where ω_1 is the fundamental frequency. Once the effective frequency of a pure ac waveform has been calculated, the effective frequency with a dc component can be calculated by a reapplication of (26)

$$\omega_{\text{eff}} = \sqrt{\frac{I_{\text{ac}}^2 \omega_{\text{eff-ac}}^2}{I_{\text{dc}}^2 + I_{\text{ac}}^2}}. \quad (27)$$

Finding Fourier coefficients and then summing the infinite series in (26) can be tedious. A shortcut, suggested but not fleshed out in [9], can be derived by noting that

$$\sum_{j=0}^{\infty} I_j^2 \omega_j^2 = \left[\text{rms} \left\{ \frac{d}{dt} I(t) \right\} \right]^2 \quad (28)$$

so that

$$\omega_{\text{eff}} = \frac{\text{rms} \left\{ \frac{d}{dt} I(t) \right\}}{I_{\text{tot-rms}}}. \quad (29)$$

The primary limitation of effective-frequency analysis is that it does not work for waveforms with more substantial harmonic content. For instance, the series in (26) does not converge for a square wave. Similarly, the derivative of a square wave in (29) results in an infinite rms value. A Bessel-function-based description of loss may be necessary. However, in practice leakage inductance prevents an inductive component from having perfectly square current waveforms.

A square wave with finite-slope edges leads to a finite value of ω_{eff} , which can be found from (29) to be

$$\omega_{\text{eff}} = \frac{\omega_1}{\pi} \sqrt{\frac{6}{\Delta(3-4\Delta)}} \quad (30)$$

where Δ is the transition time as a fraction of the total period. For $\Delta = 0.5$, the waveform becomes triangular and (30) gives the same value of ω_{eff} as calculated above. This expression (30) and the calculation and minimization of loss based on (2) is valid as long as there is not significant harmonic current for which the wire diameter is large compared to a skin depth. Based on the rule thumb that the highest important harmonic number is given by $N = 0.35/\Delta$ [27], a rough check on this would be to calculate skin depth for a maximum frequency $\omega_{\text{max}} = (0.35\omega_1/\Delta)$ and compare this to the wire diameter. If there are significant harmonics for which the skin depth is small compared to wire diameter, then the analysis in [27] can facilitate 1-D analysis of nonsinusoidal waveforms, or for more accuracy Bessel-function analysis [17] with a Fourier decomposition of the waveform can be used.

ACKNOWLEDGMENT

The author thanks New England Electric Wire Corporation for litz wire samples, Magnetics Division of Spang and Co. for ferrite core samples, and A. M. Tuckey for a careful reading of an earlier version of this paper.

REFERENCES

- [1] C. R. Sullivan and M. J. Powers, "A high-efficiency maximum power point tracker for photovoltaic arrays in a solar-powered race vehicle," in *23rd Annu. IEEE Power Electronics Specialists Conf.*, 1993, pp. 574–580.
- [2] S. Butterworth, "Effective resistance of inductance coils at radio frequency—Part I," *Wireless Eng.*, vol. 3, pp. 203–210, Apr. 1926.
- [3] ———, "Effective resistance of inductance coils at radio frequency—Part II," *Wireless Eng.*, vol. 3, pp. 309–316, May 1926.
- [4] S. Butterworth, "Effective resistance of inductance coils at radio frequency—Part III," *Wireless Eng.*, vol. 3, pp. 417–424, July 1926.
- [5] ———, "Effective resistance of inductance coils at radio frequency—Part IV," *Wireless Eng.*, vol. 3, pp. 483–492, Aug. 1926.
- [6] G. W. O. Howe, "The high-frequency resistance of multiply-stranded insulated wire," in *Proc. Royal Society of London*, vol. XCII, Oct. 1917, pp. 468–492.
- [7] J. Jongsma, "Minimum loss transformer windings for ultrasonic frequencies, Part 1: Background and theory," *Phillips Electronics Applications Bull.*, vol. E.A.B. 35, pp. 146–163, 1978.
- [8] ———, "Minimum loss transformer windings for ultrasonic frequencies, Part 2: Transformer winding design," *Phillips Electronics Applications Bull.*, vol. E.A.B. 35, pp. 211–226, 1978.
- [9] ———, "High frequency ferrite power transformer and choke design, Part 3: Transformer winding design," *Tech. Rep.* 207, 1986.
- [10] P. S. Venkatraman, "Winding eddy current losses in switch mode power transformers due to rectangular wave currents," in *Proc. Powercon 11*, 1984, pp. 1–11.
- [11] N. R. Coonrod, "Transformer computer design aid for higher frequency switching power supplies," in *IEEE Power Electronics Specialists Conf. Rec.*, 1984, pp. 257–267.
- [12] J. P. Vandelay and P. Ziogas, "A novel approach for minimizing high frequency transformer copper losses," in *IEEE Power Electronics Specialists Conf. Rec.*, 1987, pp. 355–367.
- [13] L. H. Dixon, Jr., "Review of basic magnetics, theory, conceptual models, and design equations," in *Unitrode Switching Regulated Power Supply Design Seminar Manual*, pp. M4–1–M4–11. Unitrode Corp., 1988.
- [14] E. C. Snelling, *Soft Ferrites, Properties and Applications*, 2nd ed. London, U.K.: Butterworth, 1988.

- [15] A. M. Urling, V. A. Niemela, G. R. Skutt, and T. G. Wilson, "Characterizing high-frequency effects in transformer windings—A guide to several significant articles," in *APEC 89*, Mar. 1989, pp. 373–385.
- [16] P. L. Dowell, "Effects of eddy currents in transformer windings," *Proc. Inst. Elect. Eng.*, vol. 113, pp. 1387–1394, Aug. 1966.
- [17] J. A. Ferreira, "Improved analytical modeling of conductive losses in magnetic components," *IEEE Trans. Power Electron.*, vol. 9, pp. 127–131, Jan. 1994.
- [18] ———, *Electromagnetic Modeling of Power Electronic Converters*. Norwell, MA: Kluwer, 1989.
- [19] A. W. Lotfi and F. C. Lee, "A high frequency model for litz wire for switch-mode magnetics," in *Conf. Rec. 1993 IEEE Industry Applications Conf. 28th IAS Annu. Meeting*, vol. 2, Oct. 1993, pp. 1169–75.
- [20] J. A. Ferreira, "Analytical computation of ac resistance of round and rectangular litz wire windings," *Proc. Inst. Elect. Eng.*, vol. 139, pp. 21–25, Jan. 1992.
- [21] B. Carsten, "High frequency conductor losses in switchmode magnetics," in *Tech. Papers of the 1st Int. High Frequency Power Conversion 1986 Conf.*, May 1986, pp. 155–176.
- [22] M. Bartoli, N. Noferi, A. Reatti, and M. K. Kazimierczuk, "Modeling litz-wire winding losses in high-frequency power inductors," in *27th Annu. IEEE Power Electronics Specialists Conf.*, vol. 2, June 1996, pp. 1690–1696.
- [23] J. Hu and C. R. Sullivan, "Optimization of shapes for round-wire high-frequency gapped-inductor windings," in *Proc. 1998 IEEE Industry Applications Society Annu. Meeting*, 1998, pp. 907–912.
- [24] National Electrical Manufacturer's Association, *Magnet Wire*, MW-1000-1997.
- [25] C. R. Sullivan, "Cost-constrained selection of strand wire and number in a litz-wire transformer winding," in *Proc. 1998 IEEE Industry Applications Soc. Annu. Meeting*, pp. 900–906.
- [26] J. Lammeraner and M. Staffl, *Eddy Currents*, G. A. Toombs, Ed. Boca Raton, FL: CRC, 1966.
- [27] J. G. Breslin and W. G. Hurley, "Derivation of optimum winding thickness for duty cycle modulated current waveshapes," in *28th Annu. IEEE Power Electronics Specialists Conf.*, vol. 1, pp. 655–661, 1997.



Charles R. Sullivan (M'93) was born in Princeton, NJ, in 1964. He received the B.S. degree in electrical engineering with highest honors from Princeton University, Princeton, NJ, in 1987 and the Ph.D. degree in electrical engineering from the University of California, Berkeley, in 1996.

From 1987 to 1990, he was with Lutron Electronics, Coopersburg, PA, developing high-frequency dimming ballasts for compact fluorescent lamps. He is presently an Assistant Professor at the Thayer School of Engineering, Dartmouth College, Hanover, NH. He has published technical papers on topics including thin-film magnetics for high-frequency power conversion, dc-dc converter topologies, energy and environmental issues, and modeling, analysis, and control of electric machines.

Dr. Sullivan received the AIME Ross N. Tucker Electronics Materials Award in 1995.